Weierstraß-Institut
für Angewandte Analysis und Stochastik
Leibniz-Institut im Forschungsverbund Berlin e. V.

Preprint ISSN 0946 – 8633

Beam shaping mechanism in spatially modulated edge emitting broad area semiconductor amplifiers

Mindaugas Radziunas[1], Muriel Botey[2], Ramon Herrero[3], Kestutis Staliunas[4,3]

submitted: May 31, 2013

[1] Weierstrass Institute
Mohrenstr. 39
10117 Berlin, Germany
E-Mail: Mindaugas.Radziunas@wias-berlin.de

[2] Departament de Física i Enginyeria Nuclear
Universitat Politècnica de Catalunya
Urgell 187
08036 Barcelona, Spain
E-Mail: muriel.botey@upc.edu

[3] Departament de Física i Enginyeria Nuclear
Universitat Politècnica de Catalunya
Colom 11
08222 Terrassa, Spain
E-Mail: ramon.herrero@upc.edu

[4] Institució Catalana de Recerca i Estudis Avançats
Pg. Lluis Companys, 23
08010 Barcelona, Spain
E-Mail: kestutis.staliunas@icrea.cat

No. 1790
Berlin 2013

2010 *Mathematics Subject Classification.* 35Q60, 35B27, 37M05, 78A60, 78A45.

2008 *Physics and Astronomy Classification Scheme.* 42.60.By, 42.60.Da, 42.60.Fc, 42.60.Jf.

Key words and phrases. Broad area semiconductor amplifier, periodic modulation, spatial modulation, angular filtering, beam shaping, far field, quality improvement, traveling wave model .

The work of M. R. was supported by DFG Research Center MATHEON "Mathematics for key technologies: Modelling, simulation, and optimization of real-world processes". M. B., R. H. and K. S. acknowledge the financial support of Spanish Ministerio de Educación y Ciencia and European FEDER (project FIS2011-29734-C02-01).

Edited by
Weierstraß-Institut für Angewandte Analysis und Stochastik (WIAS)
Leibniz-Institut im Forschungsverbund Berlin e. V.
Mohrenstraße 39
10117 Berlin
Germany

Fax: +49 30 20372-303
E-Mail: preprint@wias-berlin.de
World Wide Web: http://www.wias-berlin.de/

Abstract

We investigate beam shaping in broad area semiconductor amplifiers induced by a periodic modulation of the pump on a scale of several microns. The study is performed by solving numerically a (2+1)-dimensional model for the semiconductor amplifier. We show that, under realistic conditions, the anisotropic gain induced by the pump periodicity can show narrow angular profile of enhanced gain of less than one degree, providing an intrinsic filtering mechanism and eventually improving the spatial beam quality.

1 Introduction

Edge emitting broad area semiconductor (BAS) lasers are relevant light sources due to their numerous applications. Their particular geometry (planar configuration) provides high conversion efficiency, as the pump efficiently accesses the entire volume of the active amplifying medium. The main disadvantage of BAS lasers is the relatively low spatial and temporal quality of the emitted beam [1, 2] due to the absence of an intrinsic selection mechanism within its large aspect-ratio cavity. In addition, the Bespalov-Talanov modulation instability in strongly nonlinear regimes may lead to filamentation and additionally deteriorate the quality of the beam [3]. The multi-transverse mode operation results in a strong divergence of the emitted beam, and, among others, prevents coupling into optical fibers which precludes such lasers from many other important applications.

The typical divergence of BAS lasers emission (3–5 mm long, 200 μm wide, and wavelength around 1 μm) ranges from 5° to 10°. A great challenge would be to reduce such divergence to much less than 1°, i.e., closer to the diffraction limit (that is 0.1° for a 200 μm wide beam). Several approaches have been proposed and applied to improve the spatial quality of the radiation, each, however, with its disadvantages. For example, different schemes of optical injection [4, 5] and optical feedback [6, 7], or integrated narrow master oscillator – tapered power amplifier configurations [8, 9] improve the beam quality, however, in return, the laser becomes less compact, or is rather sensitive to the back reflections.

Recently novel techniques have been proposed to improve the spatial quality of the beams implementing a spatial (or angular) filtering mechanism in materials with spatially modulated refractive index on the wavelength scale. Photonic Crystals (PhCs) apart from being well-known for tailoring frequency dispersion [10] can also display angular band-gaps [11]. The angular positions of such band-gaps depend, among others, on the geometry of the modulation, i.e on the longitudinal and transverse periods of the PhC – $d_\parallel$ and $d_\perp$ – respectively. A dimensionless geometric parameter $\mathcal{Q} = 2d_\perp^2 n_b/(\lambda_0 d_\parallel)$ determines the character of spatial dispersion, where λ_0 is the considered beam wavelength in vacuum, and n_b is the background refractive index.

Hence, a proper selection of the geometry, satisfying $\mathcal{Q} \approx 1$, sets angular band-gaps at small angles from the optical axis direction, whereas the on-axis radiation lays in propagation bands. This results in a low-angle-pass filter recently proposed and demonstrated in optics [11, 12, 13, 14], but also in acoustics (by so called Sonic Crystals) [15, 16].

On the other hand, materials with periodically in space modulated gain have recently shown to provide anisotropic amplification profile [17, 18]. The maximum amplification is obtained for beams propagating along the crystallographic axes of the modulated structure, for the geometry factor $\mathcal{Q} = 1$, similar to PhCs angular filters. Physically, anisotropic gain for specific Bloch modes of the radiation (for a given frequency and propagation direction) is obtained when their field maxima coincide with the spatial areas of maximum gain. Therefore, such modes are more amplified than non-resonant Bloch waves, or than plane waves in a homogeneous (averaged) gain medium.

We propose here to combine both gain and index modulation (GIM) in order to obtain three in one: amplification, angular filtering and eventually improvement of the spatial structure of the beam. It has been recently proposed that a resulting anisotropic gain could be used in BAS lasers and amplifiers [19], where the proof-of-principle calculations were performed on a simplified model. The aim of the present work is to verify whether the scheme is indeed applicable to actual BAS amplifiers with realistic parameters of today-available semiconductor materials. Additional purpose is to quantify the predicted effect, and to calculate the angular width of the enhanced amplification profile. We also note that although the object of our study is not a BAS laser but a BAS amplifier, we expect that a strongly anisotropic gain in the amplifier would mean improving the beam structure of lasers too.

The geometry which we simulate is illustrated in Fig. 1. There are various possibilities to spatially modulate the BAS amplifier, such as using spatially modulated electrodes for electric pumping (as considered in the present letter), or micro-structuring the amplifying media (e. g. etching periodic arrays of holes, and possibly filling them by media with desired refraction properties).

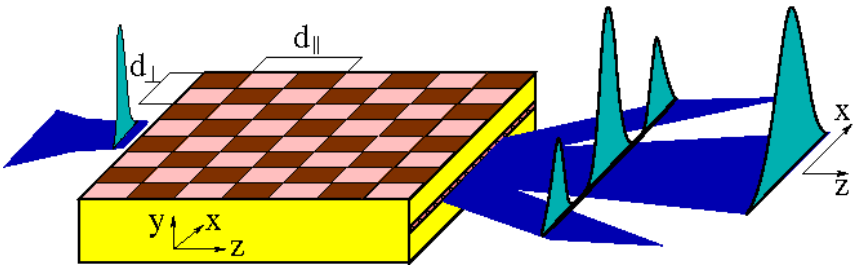

Figure 1: Planar semiconductor amplifier structure with chess-box electrodes. The pump profile is periodically modulated in space, with longitudinal and transverse periods $d_{\parallel}$ and $d_{\perp}$.

Throughout this letter, we consider a chess-box shape for the electrodes, as shown in Fig. 1. A narrow beam of a width $20\ \mu$m and corresponding divergence of 1° is injected into such a single-pass amplifier. The periodic distribution of gain in the transverse direction results in splitting the transmitted beam into at least three diffracted components as shown in Fig. 1: a central beam, and two symmetrically positioned diffraction beams, propagating at angles $\pm\varphi(d_{\perp})$. Due to the resonant interplay between transverse and longitudinal modulations of the amplifying medium,

which occurs at $\mathcal{Q} \approx 1$, these three field harmonics interact and, as a result, anisotropic gain develops. In particular we assume $\lambda_0 = 1\,\mu$m, $n_b \approx 3.125$, and in most cases $d_\perp = 8\,\mu$m, $d_\parallel = 400\,\mu$m, which fulfill the above resonance condition. The free-space diffraction angle for this case is $\varphi \approx 7.2°$. In order to determine the optimum angular filtering performance, we scan the $\mathcal{Q}$ parameter in a range around 1. Practically, to avoid redesigning the geometrical structure of the BAS amplifier for each run of computations we, instead, scan the backgroundn_b of the system.

2 Mathematical model

We use a 2+1-dimensional traveling wave model approach [9, 20, 21], where the spatio-temporal dynamics of the optical field is governed by the following set of equations:

$$\begin{aligned} &\left[\tfrac{n_g}{c_0}\partial_t + \partial_z + \tfrac{i}{2k_0 n_b}\partial_x^2\right] E = \left[\beta(N,|E|^2) - \mathcal{D}\right] E, \\ &\mathcal{D}E = \tfrac{\overline{g}}{2}\left(E - P\right), \quad \partial_t P^{\pm} = \overline{\gamma}\left(E - P\right) + i\overline{\omega}\, P, \\ &E(0,x,t) = a(x,t) = \sqrt{\tfrac{2n_g\lambda_0}{\sigma d h c_0^2}\sqrt{\tfrac{\ln 2}{\pi}}\mathcal{P}}\, e^{i\omega t - \frac{x^2 \ln 4}{\sigma^2}}, \end{aligned} \tag{1}$$

here $E(z,x,t)$ is the slowly varying complex amplitude of the optical field propagating along the longitudinal axis of the BAS amplifier, $|E|^2$ denotes a local photon density, the linear operator $\mathcal{D}$ and the induced polarization function $P(z,x,t)$ model the Lorentzian approximation of the material gain dispersion [22], whereas the complex function $a(x,t)$ represents an optically injected Gaussian beam of power $\mathcal{P}$. The complex propagation factor,

$$\beta(N,|E|^2) = -\left[\tfrac{\alpha}{2} + i\,\delta_0\right] + \tfrac{g(N,|E|^2)}{2} + i\,\tilde{n}(N), \tag{2}$$

couples the field to the carrier density $N(z,x,t)$ governed by:

$$\begin{aligned} \left[\partial_t - d_N\partial_x^2\right] N = \; & \tfrac{\bar{J}\cdot\zeta(z,x)}{qd} - (AN + BN^2 + CN^3) \\ & - \tfrac{c_0}{n_g}\Re e\left[E^*(g(N,|E|^2) - 2\mathcal{D})E\right]. \end{aligned} \tag{3}$$

The gain, the index change and the spatial current modulation functions g, $\tilde{n}$ and ζ are defined as:

$$\begin{aligned} &g(N,|E|^2) = \tfrac{g'\ln(N/N_{\rm tr})}{1+\varepsilon|E|^2}, \quad \tilde{n}(N) = k_0\sqrt{\sigma N}, \\ &\zeta(z,x) = 1 + \mathrm{sign}\left[\sin\left(2\pi z/d_z\right)\sin\left(2\pi x/d_x\right)\right]. \end{aligned} \tag{4}$$

We use the following parameters: group velocity index $n_g = 3.6$, depth of the active zone $d = 15$ nm, differential gain $g' = 25$ cm^{-1}, refractive index change factor $\sigma = 10^{-25}$ cm^3, transparency carrier density $N_{\rm tr} = 10^{18}$ cm^{-3}, internal absorption $\alpha = 1.5$ cm^{-1}, nonlinear gain compression $\varepsilon = 5\cdot 10^{-18}$ cm^3, carrier diffusion coefficient $d_N = 21$ cm^2/s, recombination parameters $A = 0.3$ 1/ns, $B = 2\cdot 10^{-10}$ cm^3/s, and $C = 2.5\cdot 10^{-30}$ cm^6/s, Lorentzian gain amplitude $\overline{g} = 100$ cm^{-1}, half width at half maximum $\overline{\gamma} = 60$ 1/ps, gain peak detuning $\overline{\omega} = 0$ 1/ps, full width at half maximum of the optical injection intensity $\sigma = 20$ μm, and mean injection current density $\bar{J} = 10$ A/mm^2. The static detuning δ and the frequency of

the optical injection ω are set to zero. Finally, c_0, q, h, and $k_0 = \frac{2\pi}{\lambda_0}$ are the speed of light in vacuum, electron charge, Planck constant, and reference wave-number, respectively. Some of these parameters are non-homogeneous, particularly, the function $\bar{J}\zeta(z,x)$ corresponds to the pump current density, which equals $2\bar{J}$ at the simulated periodic contacts and 0 elsewhere. The spatially modulated current is responsible for the modulation of the carrier density, of the propagation factor β and, therefore, for the gain and index modulation within the BAS amplifier. More details on the specific meaning and typical values of all parameters given above can be found in Ref. [9].

3 Results

The basic results are summarized in Figs. 2 and 3. Fig. 2 presents a comparison between BAS amplifiers with uniform and modulated pump. For a weak injected beam and short propagation distances ($\mathcal{P}$ = 0.1 mW and $z < 2$ mm), the propagating field has a minor impact on carrier distribution determined by the stationary Eq. (3) (see the orange curves in panels (i,j), and panels (c,d) for $z < 2$ mm). The locally averaged carrier density as well as its modulation amplitude, remain almost constant over all the width of the amplifier. Hence, the distribution of the propagation factor $\beta(z,x)$ in Eq. (1) remains defined by the stationary N. The beam intensity grows exponentially [see panels (g,h) for $z < 2$ mm] and is governed by the *linear* field equation (1) with the spatially periodic potential β. In this linear regime the far field does not change.

For $z > 2$ mm, the amplified field starts to deplete the carrier density [see panels (c,d)], which results in the saturation of the emitted field intensity [see panels (g,h)]. The amplitude of the spatial modulation of the carriers is no more uniform [see black curves in panels (i,j)], what is beyond the linear analysis of Ref. [19]. However, the predicted effects remain valid: the optical field in the modulated case develops significant side-bands at the angles $\pm\varphi(d_\perp)$, and the central far field lobe is squeezed down to $\sim 0.25^\circ$ [compare far fields for $z = 4.0$ and 5.6 mm in panels (k) and (l) and panels (e) and (f) for $z > 2$ mm].

The left column of Fig. 3 depicts the amplification properties of 4.8 mm-long devices for different values of $\mathcal{Q}$. The amplifier shows a strong narrowing of the central part of the far field for $\mathcal{Q} \in [1.01, 1.1]$ (see the contour lines in panel (a), indicating the width of the central far field lobe). The far field contains diffraction components at $\pm\varphi(8\,\mu m) \approx \pm 7.2^\circ$ [panel (e)].

For comparison, we have simulated a two times broader amplifier with the same modulation periods and same injected current density, as shown in the right column panels of Fig. 3. The narrowing of the central part of the far field is more efficient in the latter case [$\mathcal{Q} \in [1, 1.05]$ in panel (b)], however the radiation into diffraction components is also more pronounced [panel (f)] resulting in smaller part of the total radiation within the central segment [compare panels (c) and (d)].

In Fig. 4 we summarize our results for modulated BAS amplifiers with different modulation periods. In all cases, periods $d_\perp$ and $d_\parallel$ are chosen such that $\mathcal{Q} = 1.02$. It is obvious, that in the case of the smallest periods $d_\perp = 4\,\mu$m and $d_\parallel = 100\,\mu$m (black dotted curves) the compression of the central part of the far field is less pronounced (see panel (d) and panel (a) for

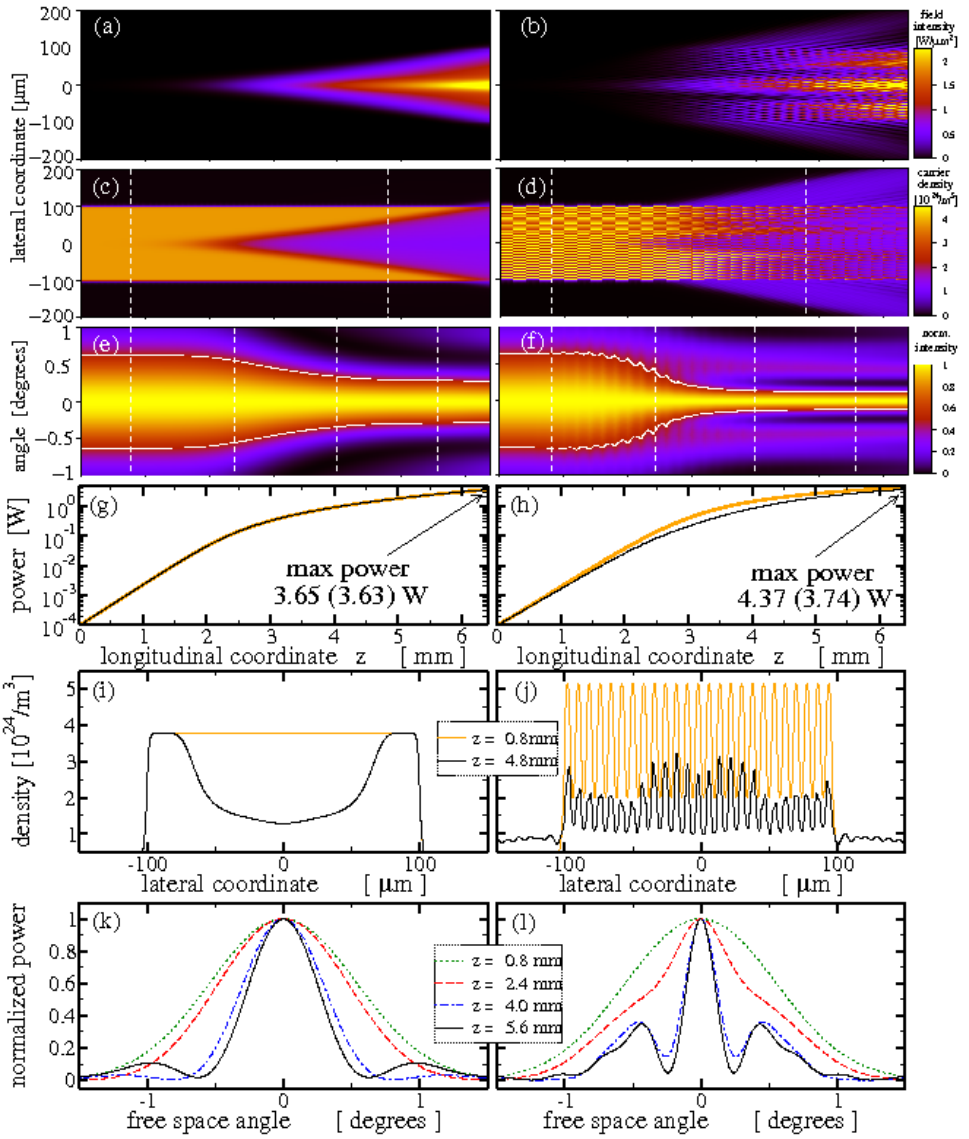

Figure 2: (color online) Amplification of the beam in $200\,\mu$m-wide BAS amplifiers for uniform pump [left column], and for periodically modulated pump with $\mathcal{Q} = 1.02$ ($n_b = 3.1875$) [right column]. From top to bottom: power (a,b); carrier densities (c,d); central part of the far field, with half maxima indicated by white contour lines (e,f); evolution of the intensity of the field [orange] and its part within the central $\pm 2.5^\circ$ segment [black] (g,h) as a function of the propagation distance, z. The carrier density and the far fields at the dashed white vertical lines of panels (c,d) and (e,f) are shown in panels (i,j) and (k,l), respectively.

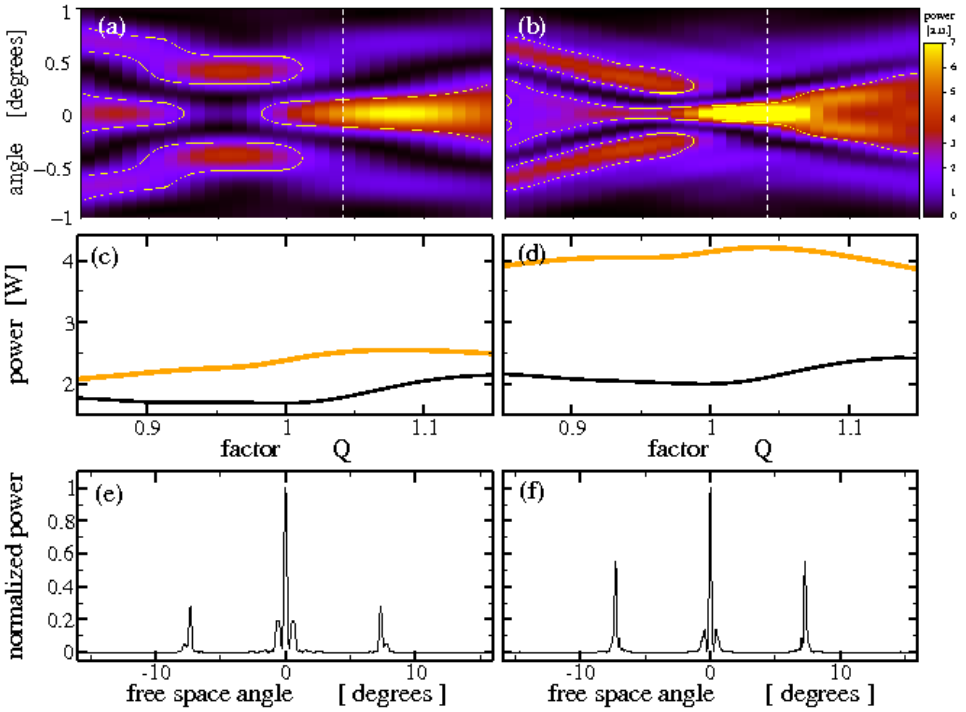

Figure 3: (color online) Amplification of the beam for a $L = 4.8$ mm long BAS amplifiers with periodical pump and two different device widths: $200\,\mu$m [left column], $400\,\mu$m [right column]. From top to bottom: central part of the far fields with half maxima indicated by light contour lines (a,b); power of the transmitted field [orange] and corresponding central part within $\pm 2.5^\circ$ [black] (c,d), as a function of $\mathcal{Q}$. The far fields for $\mathcal{Q} = 1.02$ [dashed white vertical lines in panels (a,b)] are shown in panels (e,f).

$z \leq 3.5$ mm. This can be explained by insufficient contrast of the GIM: whereas the locally averaged value of carriers (and, consequently, of gain and refractive index) in all considered cases is determined by the mean injected current $\bar{J}$, the carrier modulation and the GIM amplitudes strongly depend on the lateral period $d_\perp$ of the modulated contact. This is due to a significant contribution of the carrier diffusion, which smooths effectively the carrier distribution in devices with small modulation periods. Note also the appearance of the side lobes of the far field at $\pm 0.4^\circ$ angles [black dotted curves in panels (e) and (f)], which we attribute to the modulation instability typical for BAS amplifiers without modulation. Increasing the periods of modulation these side lobes are suppressed, and the central part of the far field is compressed down to $\sim 0.2^\circ$. On the contrary, increasing the periods of the modulation has also some drawbacks, since the optical field radiated at the angles $\pm\varphi(d_\perp)$ increases. Whereas for the case of $d_\perp = 4\,\mu$m the amount of field radiated within the central $\pm 2.5^\circ$ segment is larger than 70%, for $d_\perp = 12\,\mu$m it is less than 50% [see panel (c)], and the absolute value of this intensity is significantly lower [blue dashed curve in panel (b)]. It seems, that optimal choice of modulation periods is $d_\perp \approx 8\,\mu$m. Even though the side angle radiation is still large [red solid curve in panel (c)], the absolute amount of the emitted field within the central segment is comparable or even larger than that one in the GIM amplifier with $d_\perp = 4\,\mu$m [panel (b)], whereas the central lobe of the far field is significantly compressed [panel (d-f)].

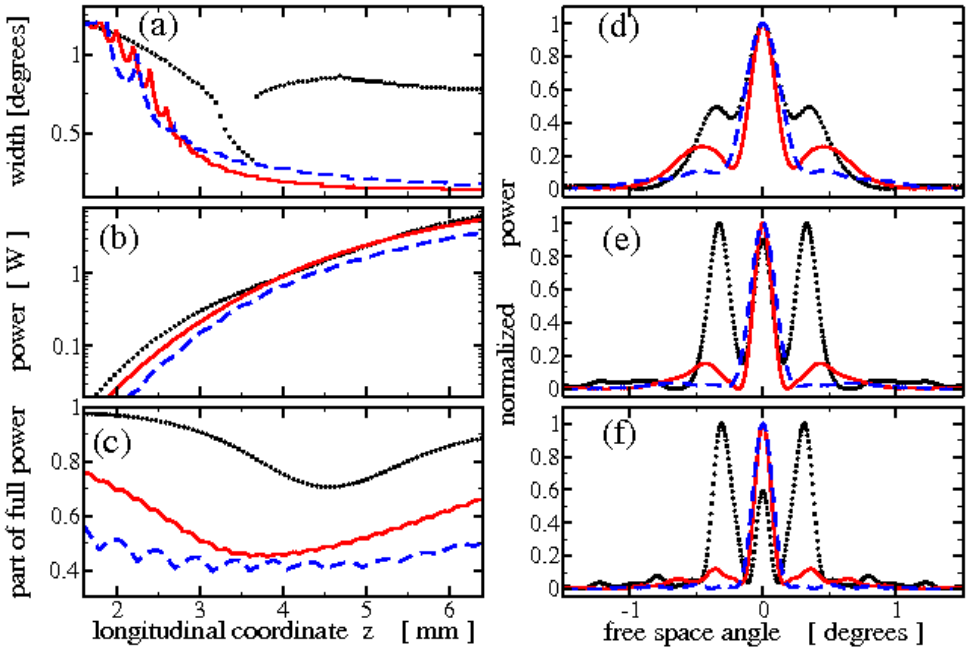

Figure 4: (color online) Amplification of the beam in $400\,\mu$m wide BAS amplifiers with modulated pump with $d_\perp = 4\,\mu$m, $d_\parallel = 100\,\mu$m (black dotted), $d_\perp = 8\,\mu$m, $d_\parallel = 400\,\mu$m (red solid), $d_\perp = 12\,\mu$m, $d_\parallel = 900\,\mu$m (blue dashed). In all three cases $\mathcal{Q} = 1.02$. (a): width of the central far field part at the half maximum. (b) and (c): intensity of the emitted field within the central $\pm 2.5^\circ$ segment and its part within the full emitted field intensity. (d), (e), and (f): central part of the far fields at $z = 3.2$ mm, $z = 4.8$ mm, and $z = 6.4$ mm, respectively.

To conclude, we show that a spatial modulation of the bias current in BAS amplifiers with a length on the order of a few millimeters can lead to a substantial improvement of the spatial structure of the amplified beam. The study is performed under realistic semiconductor parameters and technically realizable modulation periods. Beyond what is here presented, this new technique could be implemented to improve the spatial quality of emission of BAS lasers.

References

[1] T. Burkhard, M.O. Ziegler, I. Fischer, and W. Elsäßer, Chaos Soliton. Fract. **10**, 845–850 (1999)

[2] H. Adachihara, O. Hess, E. Abraham, P. Ru, and J. V. Moloney, J. Opt. Soc. Amer. B **10**, 658–665 (1993)

[3] V.I. Bespalov and V.I. Talanov, JETP Lett. **3**, 307–310 (1966)

[4] L. Goldberg and M.K. Chun, Appl. Phys. Lett. **53**, 1900–1902 (1988)

[5] M. Radziunas and K. Staliunas, Europhysics Lett. **95**, 14002 (2011)

[6] V. Raab and R. Menzel, Opt. Lett. **27**, 167–169 (2002)

[7] S.K. Mandre, I. Fischer, and W. Elsäßer, Opt. Lett. **28**, 1135 (2003)

[8] B. Sumpf, K.-H. Hasler, P. Adamiec, F. Bugge, F. Dittmar, J. Fricke, H. Wenzel, M. Zorn, G. Erbert, and G. Trankle, IEEE J. Select. Topics in Quantum Electron. **15**, 1009–1020 (2009)

[9] M. Spreemann, M. Lichtner, M. Radziunas, U. Bandelow, and H. Wenzel, IEEE J. Quantum Electron. **45**, 609–616 (2009)

[10] C.M. Soukoulis, Photonic crystals and light localization in the 21st century., Kluwer Academic Pub. **563** (2001)

[11] E. Colak, A.O. Cakmak, A.E. Serebryannikov, and E. Ozbay, J. Appl. Phys. **108**, 113106 (2010);

[12] K. Staliunas and V.J. Sánchez-Morcillo, Physical Review A **79**, 053807 (2009)

[13] L. Maigyte, T. Gertus, M. Peckus, J. Trull, C. Cojocaru, V. Sirutkaitis, and K. Staliunas, Phys. Rev. A **82**, 043819 (2010)

[14] V. Purlys, L. Maigyte, D. Gailevičius, M. Peckus, M. Malinauskas, and K. Staliunas, Phys. Rev. A **87**, 033805 (2012)

[15] R. Picó, I. Pérez-Arjona, V.J. Sánchez-Morcillo, and K. Staliunas, Appl. Acoust. **73**, 302–306 (2012)

[16] R. Picó, I. Pérez-Arjona, V.J. Sánchez-Morcillo, and K. Staliunas, Appl. Acoust. **74**, 945–948 (2013)

[17] K. Staliunas, R. Herrero, and R. Vilaseca, Phys. Rev. A **80**, 013821 (2009)

[18] M. Botey, R. Herrero, and K. Staliunas, Phys. Rev. A **82**, 013828 (2010)

[19] R. Herrero, M. Botey, M. Radziunas, and K. Staliunas, Opt. Lett. **37**, 5253–5255 (2012)

[20] S. Balsamo, F. Sartori, and I. Montroset, IEEE J. Sel. Top. Quantum Electron. **2**, 378–384 (1996)

[21] A. Egan, C.Z. Ning, J.V. Moloney, R.A. Indik, M.W. Wright, D.J. Bossert, and J.G. McInerney, IEEE J. Quantum Electron. **34**, 166–170 (1998)

[22] U. Bandelow, M. Radziunas, J. Sieber, and M. Wolfrum, IEEE J. Quantum Electron. **37**, 183–188 (2001)